

CrystEngComm

Accepted Manuscript



This is an *Accepted Manuscript*, which has been through the Royal Society of Chemistry peer review process and has been accepted for publication.

Accepted Manuscripts are published online shortly after acceptance, before technical editing, formatting and proof reading. Using this free service, authors can make their results available to the community, in citable form, before we publish the edited article. We will replace this *Accepted Manuscript* with the edited and formatted *Advance Article* as soon as it is available.

You can find more information about *Accepted Manuscripts* in the [Information for Authors](#).

Please note that technical editing may introduce minor changes to the text and/or graphics, which may alter content. The journal's standard [Terms & Conditions](#) and the [Ethical guidelines](#) still apply. In no event shall the Royal Society of Chemistry be held responsible for any errors or omissions in this *Accepted Manuscript* or any consequences arising from the use of any information it contains.

Seven Dicarboxylate-Based Coordination Polymers with Structural Varieties and Solvent Resistance Property Changing Derived from the Introduction of Small Organic Linkers

Chao Huang, Feixiang Ji, Lu Liu, Na Li, Haofei Li, Jie Wu, Hongwei Hou*, Yaoting Fan*

The College of Chemistry and Molecular Engineering, Zhengzhou University, Zhengzhou, Henan, 450052, P. R. China

* To whom correspondence should be addressed. Fax: (86) 0371-67761744;

E-mail: wujie@zzu.edu.cn

E-mail: houhongw@zzu.edu.cn

ABSTRACT: Seven new coordination polymers (CPs), namely, $\{[\text{Co}_3(\text{sdba})_3 \cdot 2\text{H}_2\text{O} \cdot \text{DMF}] \cdot 2\text{DMF}\}_n$ (**1**), $\{[\text{Co}_2(\text{sdba}) \cdot (\mu_3\text{-OH}) \cdot (\text{trz}) \cdot \text{H}_2\text{O}] \cdot \text{H}_2\text{O}\}_n$ (**2**), $\{[\text{Co}_2(\text{sdba}) \cdot (\mu_3\text{-OH}) \cdot (\text{atz}) \cdot \text{H}_2\text{O}] \cdot \text{H}_2\text{O}\}_n$ (**3**), $\{[\text{Co}(\text{sdba}) \cdot (\text{ti})_2 \cdot \text{H}_2\text{O}] \cdot 1.5\text{H}_2\text{O}\}_n$ (**4**), $\{[\text{Cu}(\text{sdba}) \cdot \text{H}_2\text{O}] \cdot 1.5\text{H}_2\text{O}\}_n$ (**5**), $\{[\text{Cu}_2(\text{sdba}) \cdot (\mu_3\text{-OH}) \cdot (\text{trz}) \cdot \text{H}_2\text{O}] \cdot \text{H}_2\text{O}\}_n$ (**6**), $\{[\text{Zn}_2(\text{sdba}) \cdot (\text{atz})_2] \cdot 0.5\text{H}_2\text{O}\}_n$ (**7**) (H_2sdba = 4,4'-sulfonyldibenzoic acid, Htrz = 1*H*-1,2,4-triazole, Hatz = 1*H*-1,2,4-triazol-3-amine, Hti = 4-(1*H*-benzo[d]imidazol-2-yl)thiazole), have been solvothermally synthesized and characterized by IR spectroscopy, elemental analysis and X-ray single-crystal diffraction. Complex **1** displays a 6-connected three-dimensional (3D) framework with $\{4^{12}.6^3\}$ **pcu** topology, which consists of two-dimensional (2D) zigzag sheets connected in an alternate fashion. Complexes **2**, **3** and **6** are isostructural, exhibiting a 8-connected “onion” 3D framework with the first reported $\{3^6.4^{10}.5^6.6^6\}$ **whc1** topology. Complex **4** exhibits a one-dimensional (1D) helix chain, which is further connected by the hydrogen bonds, giving a 2D supramolecular framework. Complex **5** reveals a 1D ∞ -like chain. Compound **7** is a 3D metal-organic framework, which shows tetranodal 3,3,4,4-*c* net with the point symbol $\{4^6.8^2.10^{12}\} \{4^6.8^3.10\} \{4^6.8\} \{4^8.2\}$ named **whc2** topology. The solvent resistance property of **1–7** has been investigated in detail. It demonstrates that with the introduction of rigid organic molecules (Htrz , Hatz , and Hti) as auxiliary ligands, complexes **2–4**, **6** and **7** show remarkable hydrothermal stability and boiling organic solvents resistance. More importantly, an alternative strategy for the rational assembly of CPs with both good solvent resistance and intriguing structural topologies has been proposed. In addition, the luminescent properties of complexes **2**, **6**, and **7** are discussed, and the thermal stabilities of complexes **2** and **7** are also investigated.

INTRODUCTION

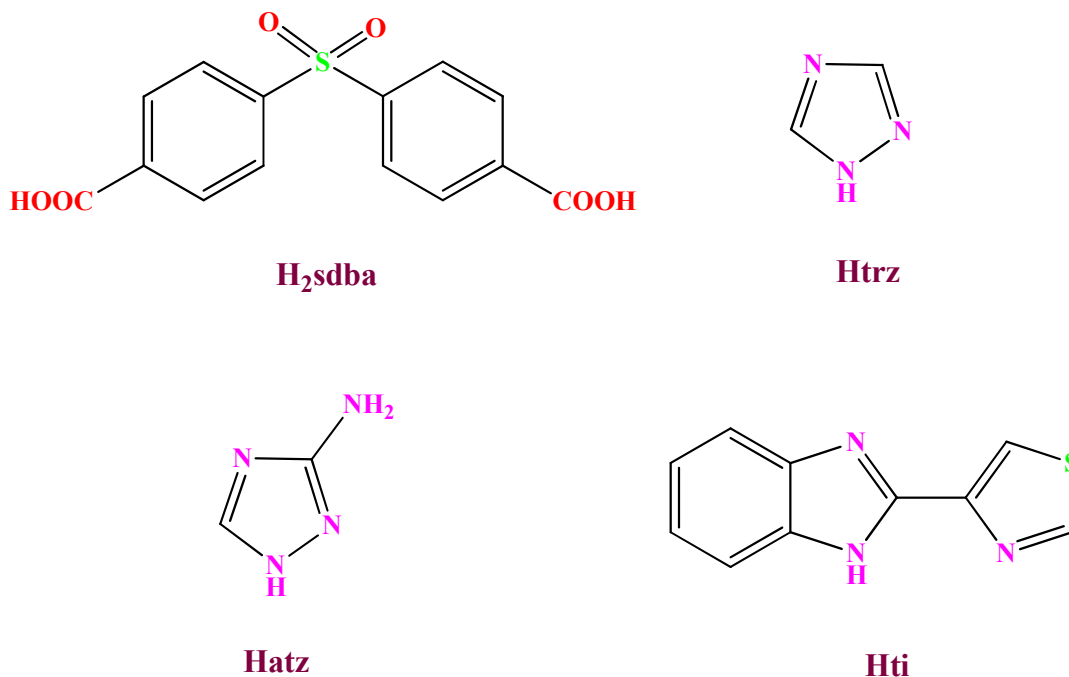
In recent years, tremendous interest has been paid to the design and synthesis of coordination polymers (CPs), stemming from not only their fascinating nature of molecular connectivities and topologies, but also their potential applications as functional materials in the areas of gas adsorption,¹

catalysis,² drug delivery,³ molecular magnetism,⁴ and photoluminescent properties.⁵ Therein, for the practical application of CPs as solid-state functional materials in single-crystal to single-crystal,⁶ separation,⁷ especially in drug delivery and heterogeneous catalysis,⁸ advantage factor, a high level of solvent resistance property is very essential to be considered. Though a large number of metal-organic coordination polymers have been prepared, it is still a challenge to search for new approaches to attain applied CPs with good solvent resistance property and predictable functional properties, because of many factors, such as the coordination geometry of the central metal ions, connective modes of organic ligands, hydrogen bonding interaction, aperture diameters, and geometric matching of the metal ions with ligand, which have great influences on the frameworks of resulting structures and the interaction of solvent and materials.⁹ It has been proposed that the organic ligands, which can meet the coordination request of metal ions with the slightest bend and twist, play important roles in determining the stability of the coordination frameworks and topologies of CPs.¹⁰ In addition, the solvent resistance property of the CPs can also be effectively improved and modulated by changing the property and aperture diameter of cavities.¹¹ The urge to synthesize CP-based materials with both high level of solvent resistance and predictable functional properties has driven the chemists to design and explore new ligands or mixed-ligands strategy capable of forming extended networks upon complexation with transition metals.

In our continuing quest to develop new strategies necessary for the rational assembly of CPs with high solvent stability and intriguing structural topologies,^{10d-10g} a rigid V-shaped bicarboxylate ligand featuring two benzoic acid groups connected by sulfonyl group, named 4,4'-sulfonyldibenzoic acid (H₂sdba), captured our attention.¹² Ligand H₂sdba, as a multidentate O-donor ligand with versatile coordination conformations and strong coordination ability, can adopt a variety of coordination modes to conform to the requirements of the coordination geometries of metal centers and, thus, result in stable diverse multidimensional architectures. It also could exhibit regular orientations with the two benzoic acid groups bent at ca. 90° arising from the distorted tetrahedral geometry of SO₂C₂.¹² The conformation is in favour of improving the stability of the formed frameworks because it can best meet the geometric

requirement of metal centers.^{10a, 13} In addition, the sulfonyl group is a fascinating functional group because it tends to form hydrogen bonds among themselves and interact negligibly with guest molecules as well as the counter anions to further stabilize the framework. Furthermore, it was anticipated that the introduction of small organic N-donor ligands (Htrz, Hatz, and Hti) into the CPs based on H₂sdba could further improve the solvent resistance property and tune structural topologies. These small organic molecules could adopt flexible bidentate chelating or bridging modes to link center metal ions and increase the number of connected nodes. Furthermore, they could also form potential hydrogen bond and decrease the aperture diameters and the intermolecular forces between the solvent and the crystals, consequentially, improving the solvent resistance property of final compounds.

Herein, as an extension of this methodology, seven new CPs based on H₂sdba and ancillary ligands (Htrz, Hatz, and Hti) (**Scheme 1**), namely $\{[\text{Co}_3(\text{sdba})_3 \cdot 2\text{H}_2\text{O} \cdot \text{DMF}] \cdot 2\text{DMF}\}_n$ (**1**), $\{[\text{Co}_2(\text{sdba}) \cdot (\mu_3\text{-OH}) \cdot (\text{trz}) \cdot \text{H}_2\text{O}] \cdot \text{H}_2\text{O}\}_n$ (**2**), $\{[\text{Co}_2(\text{sdba}) \cdot (\mu_3\text{-OH}) \cdot (\text{atz}) \cdot \text{H}_2\text{O}] \cdot \text{H}_2\text{O}\}_n$ (**3**), $\{[\text{Co}(\text{sdba}) \cdot (\text{ti})_2 \cdot \text{H}_2\text{O}] \cdot 1.5\text{H}_2\text{O}\}_n$ (**4**), $\{[\text{Cu}(\text{sdba}) \cdot \text{H}_2\text{O}] \cdot 1.5\text{H}_2\text{O}\}_n$ (**5**), $\{[\text{Cu}_2(\text{sdba}) \cdot (\mu_3\text{-OH}) \cdot (\text{trz}) \cdot \text{H}_2\text{O}] \cdot \text{H}_2\text{O}\}_n$ (**6**), $\{[\text{Zn}_2(\text{sdba}) \cdot (\text{atz})_2] \cdot 0.5\text{H}_2\text{O}\}_n$, had been synthesized under solvothermal conditions. Their structures are characterized by IR spectroscopy, elemental analysis, X-ray crystallography, and X-ray powder diffraction. Their solvent resistance property in boiling water, methanol, ethanol, acetonitrile, DMF, dilute acid and base solutions had been discussed. In addition, the luminescent properties of complexes **2**, **6**, and **7** were discussed, and the thermal stabilities of complexes **2** and **7** were also investigated.



Scheme 1. Schematic molecular structure of H₂sdba and bix ligands.

EXPERIMENTAL SECTION

Materials and Physical Measurements. All reagents and solvents were commercially available and used as received without further purification. FT-IR spectra were recorded on a Bruker-ALPHA spectrophotometer with KBr pellets in 400–4000 cm⁻¹ region. Elemental analyses (C, H, and N) were carried out on a FLASH EA 1112 elemental analyzer. Powder X-ray diffraction (PXRD) patterns were recorded using Cu K α_1 radiation on a PANalytical X'Pert PRO diffractometer. Thermal analyses were performed on a Netzsch STA 449C thermal analyzer at a heating rate of 10 °C·min⁻¹ in air. The luminescence spectra for the powdered solid samples were measured at room temperature on a Hitachi 850 fluorescence spectrophotometer. The excitation slit and emission slit were both 2.0 nm.

Synthesis of {[Co₃(sdba)₃·2H₂O·DMF]·2DMF}_n (1). A mixture of CoCl₂·6H₂O (0.028 g, 0.1 mmol), H₂sdba (0.031 g, 0.1 mmol), CH₃OH (5 mL) and DMF (5 mL) was placed in a 25 mL Teflon-lined stainless steel container. The mixture was sealed and heated at 160 °C for three days. After the mixture was cooled to ambient temperature at a rate of 5 °C/h, purple crystals of **1** were obtained with a yield of

63% (based on Co). Anal. calcd for $C_{51}H_{49}Co_3N_3O_{23}S_3$: C, 45.55 %; H, 3.67 %; N, 3.12 %. Found: C, 46.08 %; H, 3.68 %; N, 3.20 %. IR (KBr, cm^{-1}): 3076 (m), 2220 (vw), 1660 (s), 1514 (w), 1431 (w), 1205 (w), 1173 (m), 1088 (w), 878 (vw), 857 (vw), 721 (m), 667 (w), 488 (vw).

Synthesis of $\{[Co_2(sdba)(\mu_3-OH)(trz)H_2O] \cdot H_2O\}_n$ (2). A mixture of $Co(OAc)_2 \cdot 4H_2O$ (0.028 g, 0.1 mmol), H_2sdba (0.031 g, 0.1 mmol), $Htrz$ (0.007 g, 0.1 mmol), CH_3CN (5 mL) and H_2O (5 mL) was placed in a 25 mL Teflon-lined stainless steel container. The mixture was sealed and heated at 120 °C for three days. After the mixture was cooled to ambient temperature at a rate of 5 °C/h, purple crystals of **2** were obtained with a yield of 64% (based on Co). Anal. calcd for $C_{16}H_{15}Co_2N_3O_9S$: C, 35.38 %; H, 2.78 %; N, 7.74 %. Found: C, 35.33 %; H, 2.82 %; N, 7.79 %. IR (KBr, cm^{-1}): 3544 (m), 3395 (m), 3249 (m), 2254 (vw), 1622(s), 1566 (m), 1163(m), 1405 (w), 1077(m), 893 (vw), 868 (vw), 845 (vw), 619 (w), 499(vw), 437 (vw).

Synthesis of $\{[Co_2(sdba)(\mu_3-OH)(atz)H_2O] \cdot H_2O\}_n$ (3). A mixture of $Co(OAc)_2 \cdot 4H_2O$ (0.028 g, 0.1 mmol), H_2sdba (0.031 g, 0.1 mmol), $Hatz$ (0.008 g, 0.1 mmol), CH_3OH (5 mL) and H_2O (5 mL) was placed in a 25 mL Teflon-lined stainless steel container. The mixture was sealed and heated at 180 °C for three days. After the mixture was cooled to ambient temperature at a rate of 5 °C/h, purple crystals of **3** were obtained with a yield of 73% (based on Co). Anal. calcd for $C_{16}H_{16}Co_2N_4O_9S$: C, 34.42 %; H, 2.89 %; N, 10.34 %. Found: C, 34.37 %; H, 2.93 %; N, 10.40 %. IR (KBr, cm^{-1}): 3495 (m), 3386 (m), 1677 (s), 1600 (m), 1514 (w), 1410 (m), 1193 (m), 1133 (vw), 1077 (w), 868 (w), 845 (vw), 739 (m), 619 (w), 428(vw).

Synthesis of $\{[Co(sdba)(ti)H_2O] \cdot 1.5H_2O\}_n$ (4). A mixture of $Co(OAc)_2 \cdot 4H_2O$ (0.028 g, 0.1 mmol), H_2sdba (0.031 g, 0.1 mmol), Hti (0.020 g, 0.1 mmol), CH_3OH (5 mL) and H_2O (5 mL) was placed in a 25 mL Teflon-lined stainless steel container. The mixture was sealed and heated at 170 °C for three days. After the mixture was cooled to ambient temperature at a rate of 5 °C/h, purple crystals of **4** were obtained with a yield of 73% (based on Co). Anal. calcd for $C_{24}H_{19}CoN_3O_{8.5}S_2$: C, 47.37 %; H, 3.14 %; N, 6.91 %. Found: C, 46.19 %; H, 2.95 %; N, 6.79 %. IR (KBr, cm^{-1}): 3481 (m), 3095 (s), 2963 (w),

1592 (s), 1542 (s), 1424 (s), 1291 (m), 1160 (w), 1100(w), 873(vw), 835(vw), 745 (w), 618 (vw), 579(vw), 482(vw).

Synthesis of $\{[\text{Cu}(\text{sdba})\cdot\text{H}_2\text{O}]\cdot 1.5\text{H}_2\text{O}\}_n$ (5). A mixture of $\text{CuCl}_2\cdot 2\text{H}_2\text{O}$ (0.017 g, 0.1 mmol), H_2sdba (0.031 g, 0.1 mmol), CH_3CN (4 mL) and H_2O (4 mL) was placed in a 25 mL Teflon-lined stainless steel container. The mixture was sealed and heated at 130 °C for three days. After the mixture was cooled to ambient temperature at a rate of 5 °C/h, blue crystals of **5** were obtained with yield of 52% (based on Cu). Anal. calcd for $\text{C}_{14}\text{H}_{13}\text{CuO}_{8.5}\text{S}$: C, 40.72 %; H, 3.17 %. Found: C, 40.58 %; H, 2.99 %. IR (KBr, cm^{-1}): 3056 (m), 2160 (vw), 1680 (s), 1534 (w), 1401 (w), 1195 (w), 1173 (m), 1062 (w), 868 (vw), 847 (vw), 746 (m), 641 (w), 464 (vw).

Synthesis of $\{[\text{Cu}_2(\text{sdba})\cdot(\mu_3\text{-OH})\cdot(\text{trz})\cdot\text{H}_2\text{O}]\cdot\text{H}_2\text{O}\}_n$ (6). A mixture of $\text{Cu}(\text{NO}_3)_2\cdot 3\text{H}_2\text{O}$ (0.024 g, 0.1 mmol), H_2sdba (0.031 g, 0.1 mmol), Htrz (0.007 g, 0.1 mmol), CH_3OH (9 mL) and H_2O (1 mL) was placed in a 25 mL Teflon-lined stainless steel container. The mixture was sealed and heated at 160 °C for three days. After the mixture was cooled to ambient temperature at a rate of 5 °C/h, blue crystals of **6** were obtained with a yield of 64% (based on Co). Anal. calcd for $\text{C}_{16}\text{H}_{15}\text{Cu}_2\text{N}_3\text{O}_9\text{S}$: C, 34.78 %; H, 2.74 %; N, 7.61 %. Found: C, 34.74 %; H, 2.80 %; N, 7.67 %. IR (KBr, cm^{-1}): 3494 (m), 3375 (m), 3149 (m), 2224 (vw), 1662(s), 1506 (m), 1143(m), 1385 (w), 1007(m), 853 (vw), 828 (vw), 745 (vw), 649 (w), 489(vw), 457 (vw).

Synthesis of $\{[\text{Zn}_2(\text{sdba})\cdot(\text{atz})_2]\cdot 0.5\text{H}_2\text{O}\}_n$ (7). A mixture of $\text{ZnSO}_4\cdot 6\text{H}_2\text{O}$ (0.028 g, 0.1 mmol), H_2sdba (0.1 mmol), Hatz (0.008 g, 0.1 mmol), CH_3OH (5 mL) and H_2O (5 mL) was placed in a 25 mL Teflon-lined stainless steel container. The mixture was sealed and heated at 160 °C for three days. After the mixture was cooled to ambient temperature at a rate of 5 °C/h, colorless crystals of **7** were obtained with a yield of 73% (based on Zn). Anal. calcd for $\text{C}_{18}\text{H}_{15}\text{N}_8\text{O}_{6.5}\text{SZn}_2$: C, 35.43 %; H, 2.48 %; N, 18.36 %. Found: C, 35.37 %; H, 2.52 %; N, 18.42 %. IR (KBr, cm^{-1}): 3444 (m), 3365 (m), 3149 (m), 2054 (vw), 1672(s), 1556 (m), 1463(m), 1405 (w), 1007(m), 883 (vw), 858 (vw), 838 (vw), 599 (w), 489(vw), 457 (vw).

Crystal Data Collection and Refinement. The data of the **1–7**, were collected on a Rigaku Saturn 724 CCD diffractometer (Mo- $K\alpha$, $\lambda = 0.71073 \text{ \AA}$) at temperature of $20 \pm 1 \text{ }^\circ\text{C}$. Absorption corrections were applied by using multi-scan program. The data were corrected for Lorentz and polarization effects. The structures were solved by direct methods and refined with a full-matrix least-squares technique based on F^2 with the SHELXL-97 crystallographic software package.¹⁴ The hydrogen atoms were placed at calculated positions and refined as riding atoms with isotropic displacement parameters. The distribution of peaks in the channels of **1–7** was chemically featureless to refine using conventional discrete-atom models. To resolve these issues, the contributions of the electron density by the remaining DMF and water molecules in **1**, the water molecules in **2–7** were removed by SQUEEZE routine in PLATON.¹⁵ Final formulas were determined by combing single-crystal structures, elemental microanalyses, TGA and the electron count of the SQUEEZE results. Crystallographic crystal data and structure processing parameters for **1–7** and parts of complexes under specific conditions are summarized in Table 1. Selected bond lengths and bond angles for **1–7** and parts of complexes under specific conditions are listed in Table S1 (Supporting Information), respectively. Crystallographic data for **1–7** have been deposited at the Cambridge Crystallographic Data Centre with CCDC reference numbers 960060–960066.

Please insert Table 1 close to here

RESULTS AND DISCUSSION

Crystal Structure of 1. Single crystal X-ray diffraction analysis reveals that complex **1**, which crystallizes in the monoclinic space group $P2_1/c$, is a 3D coordination framework. Its asymmetric unit contains three Co(II) ions, three sdba^{2-} groups, one DMF molecule and two coordinated water molecules. As illustrated in Figure 1a, there are three unique Co(II) centers with the different coordination environment. Co1 ions possess typical six-coordinated octahedral coordination geometry, which is coordinated by six oxygen atoms from six sdba^{2-} ligands. Co2 is coordinated by four oxygen

atoms from three sdba^{2-} ligands, one oxygen atom from DMF molecule and one oxygen atom from coordinated water molecule, showing a distorted octahedral arrangement. While the Co3 is a distorted tetrahedral coordination geometry, which is coordinated by three oxygen atoms from three sdba^{2-} ligands, one oxygen atom from coordinated water molecule. The distances of Co–O are 1.938(5)–2.294(12) Å, which is within the normal ranges.¹⁶

All the carboxyl groups from H_2sdba ligands are deprotonated and adopt two different coordination modes. One carboxyl group takes a bisonodetate coordination mode to link two Co centers (Co1 and Co3) while the other carboxyl group adopts cheating/bridging bidentate coordination mode to bridge two Co centers (Co1 and Co2) (Figure 1b). The coordination modes are different from that of $[\text{Zn}_3(\mu\text{-OH})_2(\text{sdba})_2]_n \cdot 2n\text{H}_2\text{O}$, in which the H_2sdba ligands adopt a $(\kappa^1-\kappa^1)-(\kappa^1-\kappa^1)-\mu_4$ coordination mode with the torsional angle between the two phenyl rings being 81.441° .¹⁷ Three Co atoms are joined by three sdba^{2-} ligands to form a trinuclear Co(II) cluster as a secondary building unit (SBU) with Co2...Co1...Co3 distance of 3.492 and 3.658 Å, respectively. These SBUs can be further extended by carboxylate groups of the sdba^{2-} ligands to give a 2D zigzag sheet, in which the two benzene rings bent at ca. $103.2(4)$ – $103.8(3)^\circ$ (C5–S1–C8, C19–S2–C22, and C36–S3–C39) (Figure S1). Interestingly, the sheets are connected in an alternate fashion by Co1 atoms to generate a 3D framework without obvious cavity (Figure 1c). From the topological point of view, if the trinuclear Co(II) cluster are regarded as a connected node and the ligands are considered as linker, the structure of **1** can be described as a 6-connected **pcu** topology with the point symbol of $(4^{12}.6^3)$ (Figure 1d).

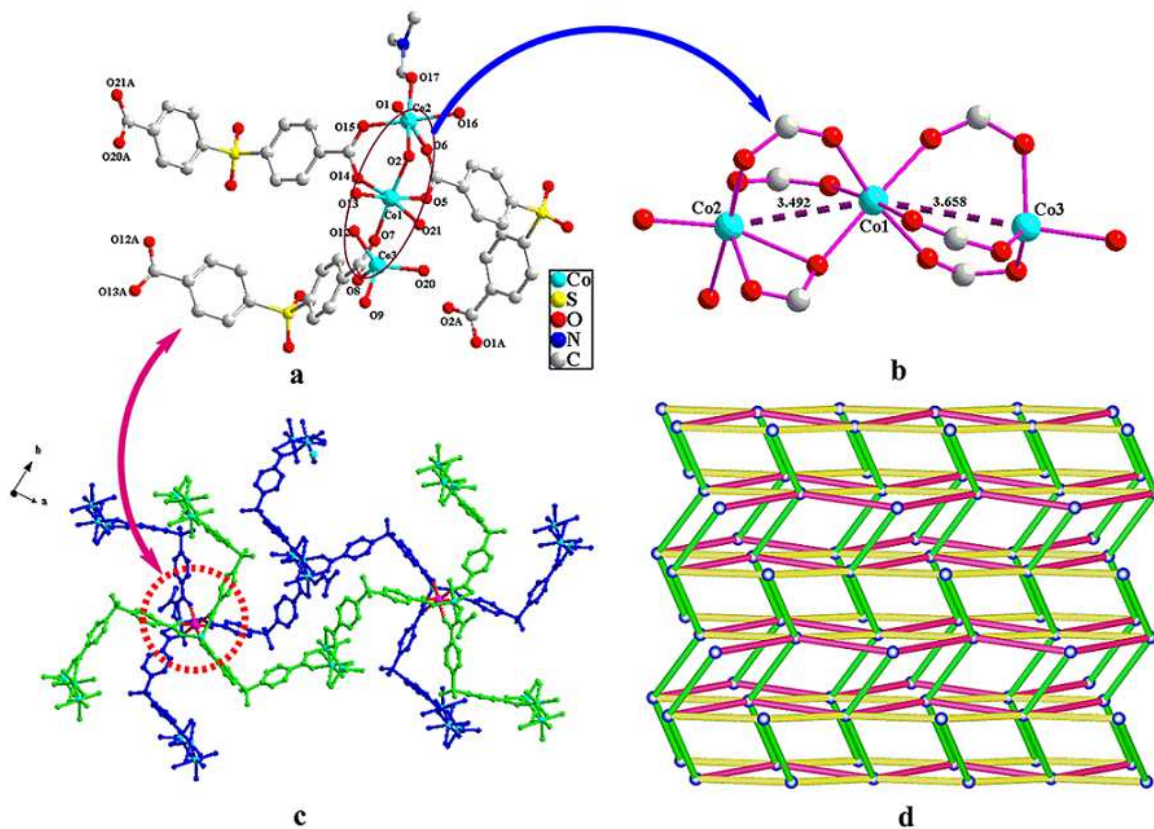


Figure 1. (a) Coordination environments of the Co(II) ions in **1**. Hydrogen atoms are omitted for clarity. (b) The coordination mode of sdba^{2-} and secondary building unit (SBU). (c) The 3D sheet are connected by Co1 (pink) to form a 3D framework. (d) Topological structure of the 3D framework.

Crystal Structure of 2. Compared with **1**, the structure of **2** had changed enormously when importing Htrz. Compound **2** crystallizes in the Tetragonal space group $I4(1)/a$ and contains an interesting 3D “onion” polymeric architecture. The asymmetric unit consists of two Co(II), one coordinated sdba^{2-} ligand, one deprotonated trz^- group, one coordinated water molecule and one $\mu_3\text{-OH}$ group, as shown in Figure 2a. The central Co1 ion has a slightly distorted trigonal bipyramid coordination geometry with two oxygen atoms (O4A and O8) from two sdba^{2-} ligands, two oxygen atoms (O1 and O1A) from two $\mu_3\text{-OH}$ groups and one nitrogen atom (N3) from one deprotonated trz^- group. Co2 ion is six-coordinated by two oxygen atoms (O3 and O7) from two sdba^{2-} ligands, one oxygen (O2) from coordinated water molecule, one oxygen atom (O1) from $\mu_3\text{-OH}$ and two nitrogen atoms (N1 and N2) from two deprotonated trz^- groups. The Co–O bond distances vary in the range of 2.010(3)–2.196(3) Å, and the Co–N bond distances vary in the range of 2.018(3)–2.089(3) Å.

As shown in Figure 2b, two pairs of symmetry-related Co(II) atoms (Co1, Co1A; Co2, Co2A) are bridged together by two μ_3 -hydroxides to form a $[\text{Co}_4(\mu_3\text{-OH})_2]$ cluster (Co \cdots Co 3.167-3.631 Å, Co–O–Co 79.20-117.59 Å) as a tetranuclear Co(II) SBU. These SBUs can be further extended by triazole groups and carboxylate groups of the symmetrical sdba^{2-} ligands. The coordination mode of ligand H_2sdba was different from **1**. All carboxyl groups from H_2sdba are deprotonated and adopt a bimonodentate coordination mode to bridge Co1 and Co2 of tetracobalt SBU with the distances of 3.630 Å for Co1 \cdots Co2, generating a 3D framework (Figure S2). The two benzene rings bent at ca. 103.1(2)° (C7–S1–C10). Moreover, each trz^- unit act as bridging linker and connect with the neighboring tetracobalt clusters to further stabilize the 3D framework (Figure 2c). Compound **2** possesses 1D channels (void = 18.6%) along *c* axis and all trz^- groups point to the square-shape channels, with the maximum and minimum aperture diameters of 3.8 and 2.9 Å, respectively.

From the topological point of view, if the trinuclear Co(II) cluster is regarded as a connected node, this tetracobalt SBU can be defined as unondal 8-connected node, and the carboxylate acts as 2-connected linkers and triazole acts as 2-connected linkers. Topological analysis shows that the Schläfli symbol for this network is $\{3^6.4^{10}.5^6.6^6\}$ named **whc1** topology (Figure 2d). This topology has been theoretically expected but not yet observed prior to this work.

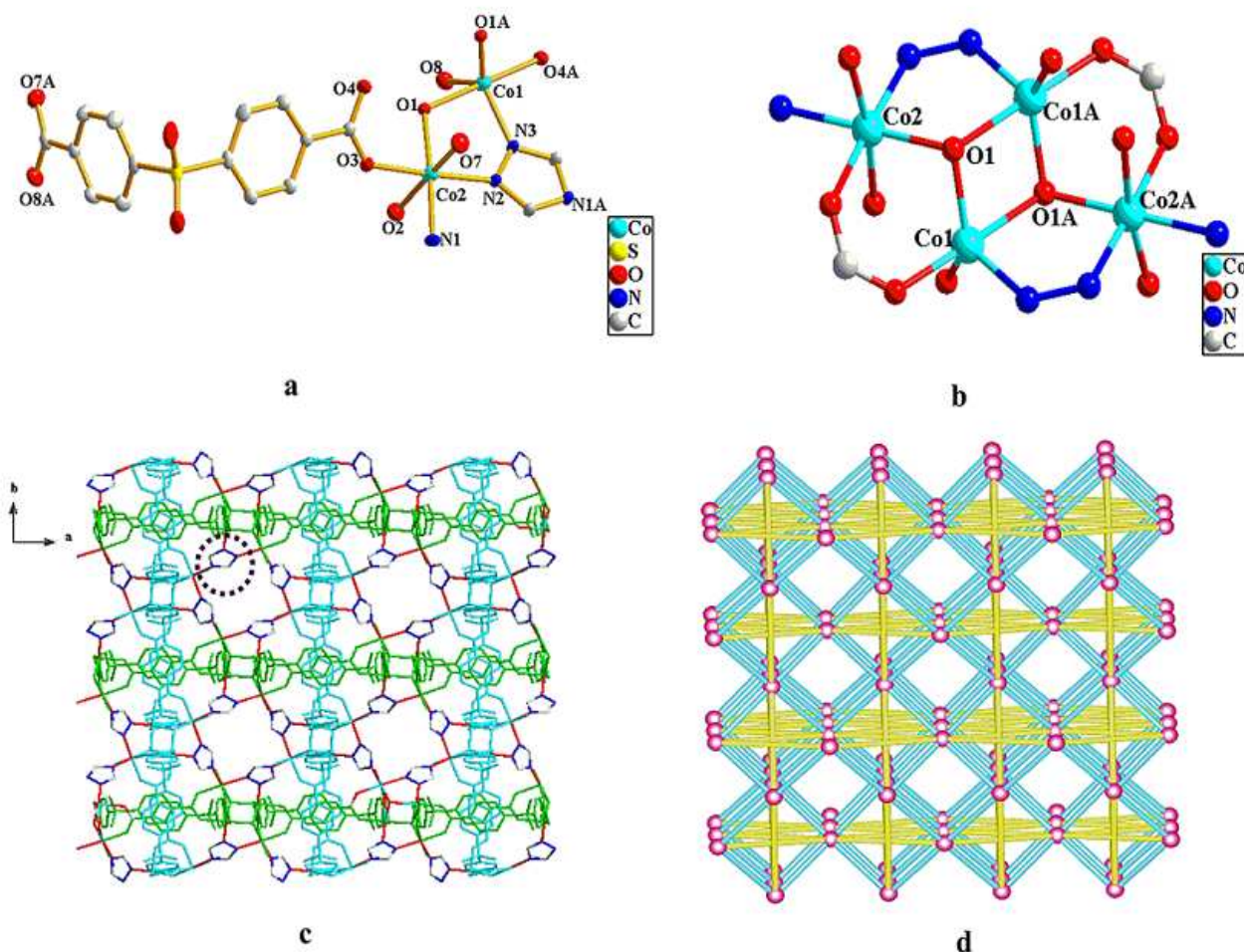


Figure 2. (a) Coordination environments of the Co(II) ions in **2**. Hydrogen atoms are omitted for clarity. (b) The tetranuclear cobalt (II) cluster. (c) Connectivity between two sheets through trz^- unit to form the 3D framework along the c axis. (d) Schematic view of the $\{3^6.4^{10}.5^6.6^6\}$ topology (the tetranuclear cobalt cluster represented as rose red ball mode).

Crystal Structure of 3. In consideration of the fact that Hatz is similar with Htrz and contains a specific $-\text{NH}_2$ group to form fascinating hydrogen bond, complex **3** was obtained when Hatz was utilized in place of Htrz under appropriate reaction conditions. The single crystal X-ray analysis shows that complex **3** is isostructural with **2**. Similar to **2**, the two pairs of Co(II) atoms are linked together by two μ_3 -hydroxides to construct a $[\text{Co}_4(\mu_3\text{-OH})_2]$ cluster as a tetranuclear Co(II) SBU. The SBUs are bridged by atz^- groups and H_2sdba with the two benzene rings bent at ca. $103.1(5)^\circ$ (C5–S1–C8) to form a 3D “onion” framework. (Figure S3). Compound **3** possesses 1D channels along c axis. All atz^- groups

point to the channel and the hydrogen atoms of amino groups are exposed on the pore surface, which further decreasing the aperture diameters. As expected, the hydrogen-bonding interactions [$N4\cdots O8 = 2.999(12)$ and $N4\cdots N3 = 3.129(12)$] were formed by $-NH_2$ group, which further stabilize the framework (Table S2).

Crystal Structure of 4. In contrast with **1**, **2**, and **3**, single crystal X-ray analysis shows that complex **4** crystallizes in monoclinic crystal system space group $C2/c$, indicating a 1D helix chains when bidentate chelating ligand Hti is imported. The asymmetric unit contains one Co(II) cation, one H_2sdba ligand, one Hti and one coordinated water molecule.

The Co(II) is surrounded by three oxygen atoms (O1, O2 and O6) from two $sdba^{2-}$ groups, two nitrogen atoms (N1 and N3) from Hti and one oxygen atom (O7) from water molecule, giving a distorted octahedral coordination geometry (Figure 4a). The carboxylate groups of the ligands connect the adjacent Co(II) cations to form a single-strand helix chain with the $Co\cdots Co$ distance of $13.1562(36)$ Å (Figure 4b). The two benzene rings bent at ca. $104.9(2)^\circ$ (C5–S1–C8). In addition, the adjacent 1D helix chains are further bridged by hydrogen-bonding interactions [$O7\cdots O5 = 2.836(5)$ Å] (Table S2) between the oxygen atoms of coordination water molecule and the adjacent uncoordination oxygen atoms from the ligands to give a two-dimensional (2D) supramolecular framework (Figure 4c). PLATON analysis gives the free void volume ratio of 11.5 % in compound **4**.

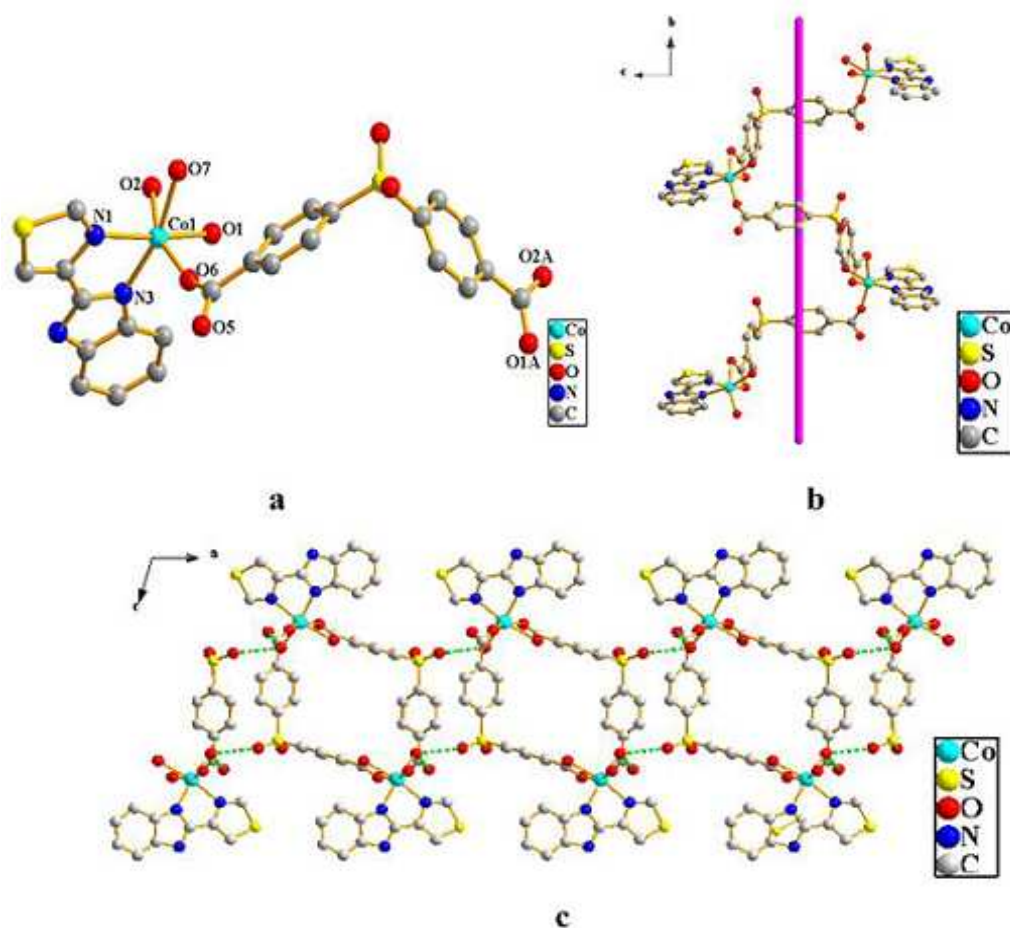


Figure 3. (a) Coordination environments of the Co(II) ions in **4**. Hydrogen atoms are omitted for clarity. (b) View of 1D helical chain along *a* axis. (c) View of the 2D network of compound **4** along *b* axis. The inter-chain strong hydrogen bonds are represented by dashed lines.

Crystal Structure of 5. Complex **5** crystallizes in the monoclinic space group $C2/m$ and exhibits a 1D ∞ -like chains. The asymmetric unit contains one Cu(II), one $sdba^{2-}$ and one coordinated water molecule. The Cu(II) atom is coordinated by four oxygen atoms from four $sdba^{2-}$ [Cu–O1 = 1.961(3) and Cu–O2 = 1.959(3) Å] and one oxygen atom from one coordinated water molecule [Cu–O4 = 2.184(51) Å], giving a distorted square pyramidal coordination geometry, where the O4 atom locates at the top of the square pyramid and the four carboxylate oxygen atoms frame the bottom (Figure S4). The fully deprotonated H_2sdba ligand indicates a bidentate coordination mode and the pairs of Cu(II) cations are linked by two symmetrical $sdba^{2-}$ ligands to form a dinuclear Cu(II) “paddlewheel” type SBU with a Cu···Cu space of 2.6244(15) Å. These SBUs are further crossed through the second terminal

carboxylate group of the symmetrical sdba^{2-} ligands into 1D chains (Figure 4a). Furthermore, there exist weak $\pi\cdots\pi$ stacking interactions (centroid-to-centroid distance of 3.8549(7) Å) among adjacent aromatic cycles of sdba^{2-} ligands, which give a two-dimensional (2D) supramolecular framework (Figure 4b). PLATON analysis gives the free void volume ratio of 18.3 % in compound **5**.

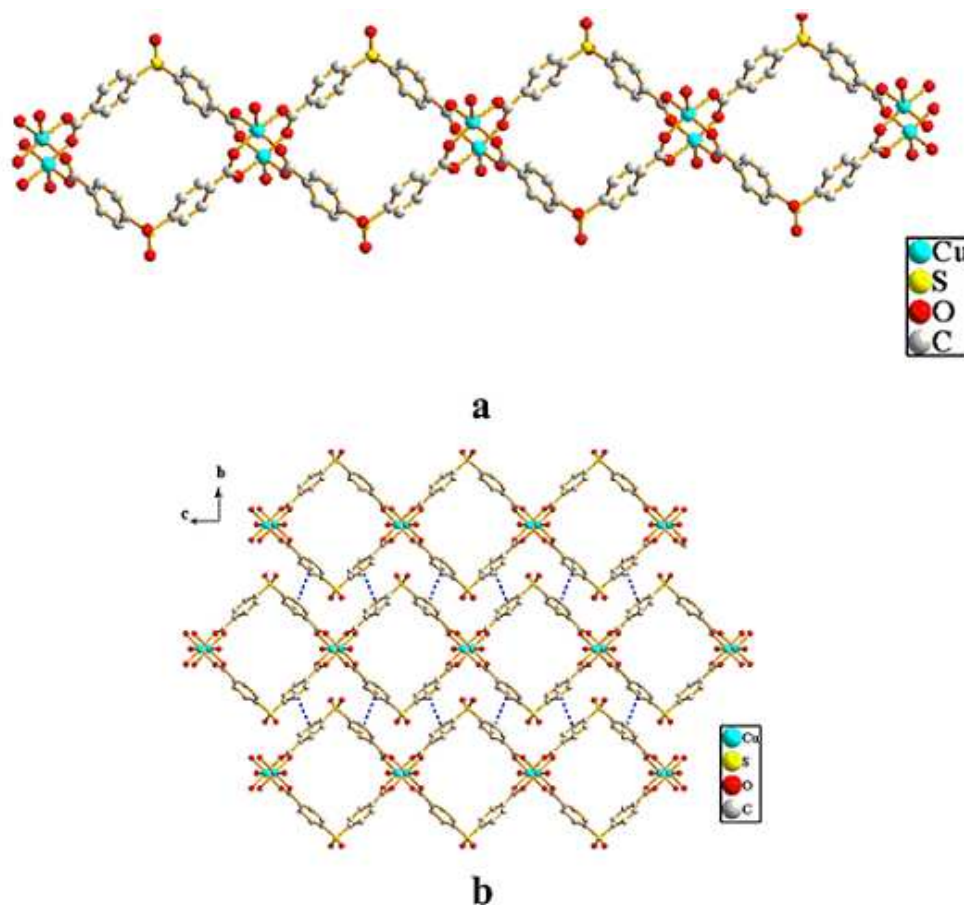


Figure 4. (a) An infinite 1D ∞ -like chains formed by Cu(II) cation centers and sdba^{2-} ligands. Hydrogen atoms are omitted for clarity. (b) View of the 2D network of compound **5** down a axis. The weak $\pi\cdots\pi$ stacking interactions are represented by dashed lines.

Crystal Structure of 6. Crystal structure determination reveals that **6** crystallizes in the Tetragonal space group $I4(1)/a$, is isostructural with **2**. Two pairs of symmetry neighbored Cu(II) atoms are connected together by two μ_3 -hydroxides to develop a $[\text{Cu}_4(\mu_3\text{-OH})_2]$ cluster as a tetranuclear Cu(II) SBU. Each tetranuclear Cu(II) SBU is joined by four completely deprotonated H_2sdba ligands and trz^- units to form a 3D framework. Compound **6** possesses 1D channels (void = 18.6%) along c axis and all

trz⁻ groups point to the square-shape channels, with the maximum and minimum aperture diameters of 3.5 and 2.8 Å, respectively.

Crystal Structure of 7. Complex 7 crystallizes in the orthorhombic space group Pbcn and exhibits a 3D coordination framework consisting of Zn-triazolate layers and dicarboxylate pillars. Its asymmetric unit contains two independent Zn(II) ions, one sdba²⁻ ligand and two atz⁻ ligands (Figure 5a). Zn1 atom is four-coordinated by three nitrogen atoms (N1, N6 and N7) from three atz⁻ ligands, one carboxylate oxygen atom (O2) from one sdba²⁻ ligand, conforming a distorted tetrahedral geometry. Zn2 atom is also tetrahedrally coordinated by three nitrogen atoms (N4, N5 and N8) from three atz⁻, one carboxylate oxygen atom (O6) from one sdba²⁻ ligand. The Zn–N bond length is vary 1.985 to 2.022 Å, and the Zn–O bond length is 1.931 and 1.954 Å, which are in the normal ranges in both cases.¹⁸ As shown in Figure 5b, the Zn(II) cations are linked through the atz⁻ ligands to form a 2D layer structure. Such layers are further bridged by bent dicarboxylate pillars, in which the two carboxylate groups adopt a monodentate coordination mode, leading to the formation of a 3D framework (Figure 5c). In order to better understand the whole structure, we can simplify the intricate structure as node-and-connecting nets. Hence, from the viewpoint of structural topology, each Zn(II) unit can be viewed as a 4-connected node, the sdba²⁻ ligand acts as a linear linker and each Htaz ligand can be reduced to a 3-connected node. So the whole framework possesses a new tetranodal 3,3,4,4-*c* net with the point symbol {4⁶.8².10¹²} {4⁶.8³.10} {4⁶.8} {4⁸.2} named **whc2** topology. (Figure 5d). In addition, these 3D framework are further stabilized by hydrogen bonds (N2⋯O1 = 2.834(6), N6⋯O2 = 2.984(6), N6⋯O6 = 2.964(6), N2⋯O2 = 3.279(6)), which is formed by –NH₂ group and oxygen atoms of carboxylate group (Table S2). PLATON analysis gives the free void volume ratio of 18.2 % in compound 7.

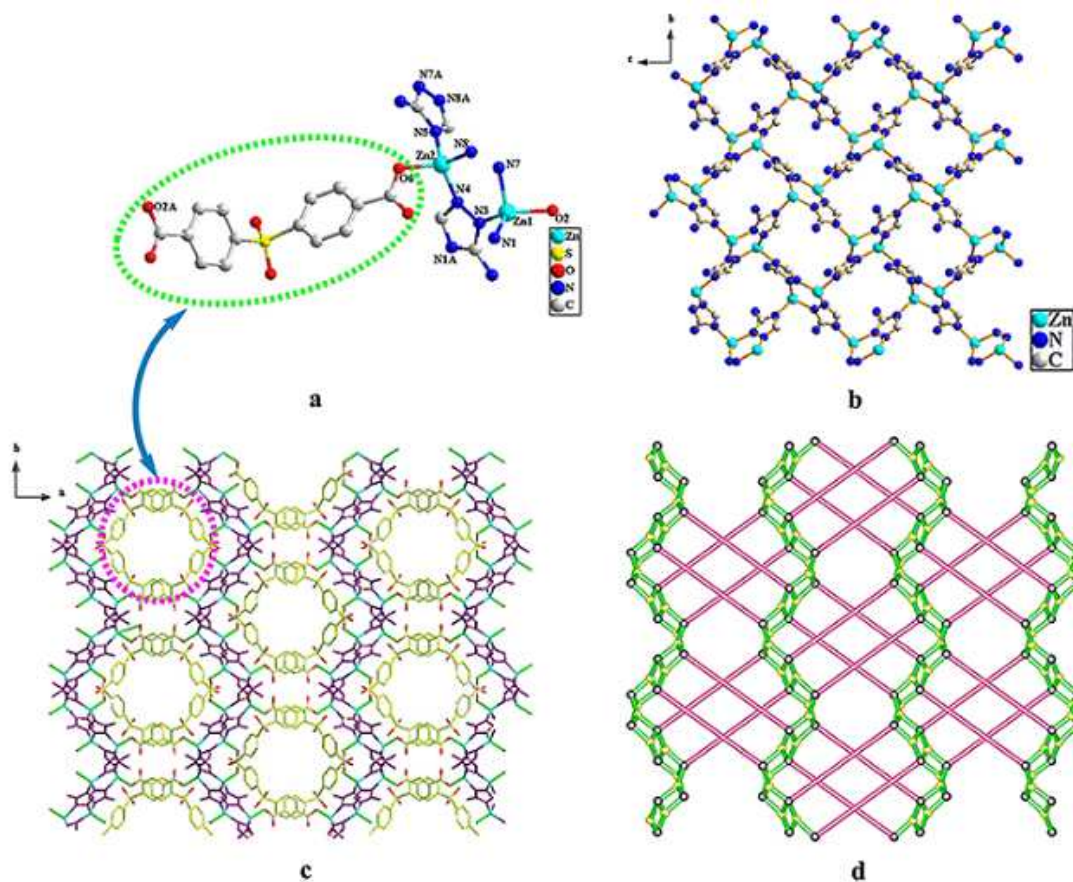


Figure 5. (a) Coordination environments of the Zn(II) ions in **7**. Hydrogen atoms are omitted for clarity. (b) View of the 2D network formed by atz^- ligands and Zn(II) cations in **7**. (c) Connectivity between two networks through sdba^{2-} unit to form the 3D framework along the c axis. (d) Schematic representation of 4-connected topology of **7** (purple nodes: Zn; yellow nodes: Hatz ligands).

Analyses of solvent resistance property. The solvent resistance property of the complexes **1–7** was examined by suspending samples in boiling water, methanol, ethanol, acetonitrile, DMF, dilute acid and base for 48 h, which imitated the typical industrial chemical processes. During this process, samples were regularly observed under an optical microscope.

It was found that the crystals of complex **1** could keep their original shapes in boiling organic solvents conditions for more than 48 h and dissolved in boiling water (Table 2). Complex **5** dissolved in boiling methanol, ethanol, and DMF conditions and could just keep the original shapes under boiling water and

acetonitrile for 48h. Single crystal X-ray diffraction showed the unit cell parameters of complexes **1** and **5** after treatment basically did not change (Table S3). Complexes **1** and **5** were directly assembled by metal ion with H₂sdba. The solvent resistance property of **1** in boiling organic solvents can be ascribed to the rigidity of the linker, dense structure, and its stable 3D framework without obvious cavity. In addition, the ligand is a rigid V-shaped linker with different coordination modes to meet with the requirements of coordination geometries of the center metal ions and provides a “pi-pocket” formed by two phenyl rings and rules the stability of the final structures.¹⁹ As to **5**, its macrocyclic subunits are liable to be attacked by solvent molecules (Figure 6).

Please insert Table 2 close to here

Complexes **2–4** were prepared by the self-assembly of Co(II) ion, H₂sdba, with Htrz, Hatz, and Hti, respectively. The structure of **2** and **3** showed a 8-coonected 3D metal-organic framework with new {3⁶.4¹⁰.5⁶.6⁶} topology, due to the bridging effect of the auxiliary ligands. Complex **4** showed a 1D helix chains. Compared with **1**, the crystals of complexes **2–4** could keep their original shapes under boiling methanol, ethanol, acetonitrile, DMF and water more than 4 days. Single X-ray diffraction studied that their unit cell parameters basically did not change (Table S4). That is to say, complexes **2–4** have more excellent boiling water and organic solvents resistance than that of **1**. This may due to the introduction of small organic N-donor ligands (Htrz, Hatz, and Hti) into the framework, which could further improve the skeleton stability. The small organic N-donor ligands (Htrz, Hatz, and Hti) could adopt bridging and bidentate chelating modes to link the center metal ions, increase the coordination number of the center metal ions, and tune structural topologies. More importantly, the organic N-donor ligands point to the channels of CPs, occupy the cavity, form hydrogen bonds and decrease the aperture diameters, which will reduce the interaction between the solvent and the crystals and prevent the dissolution of the frameworks.

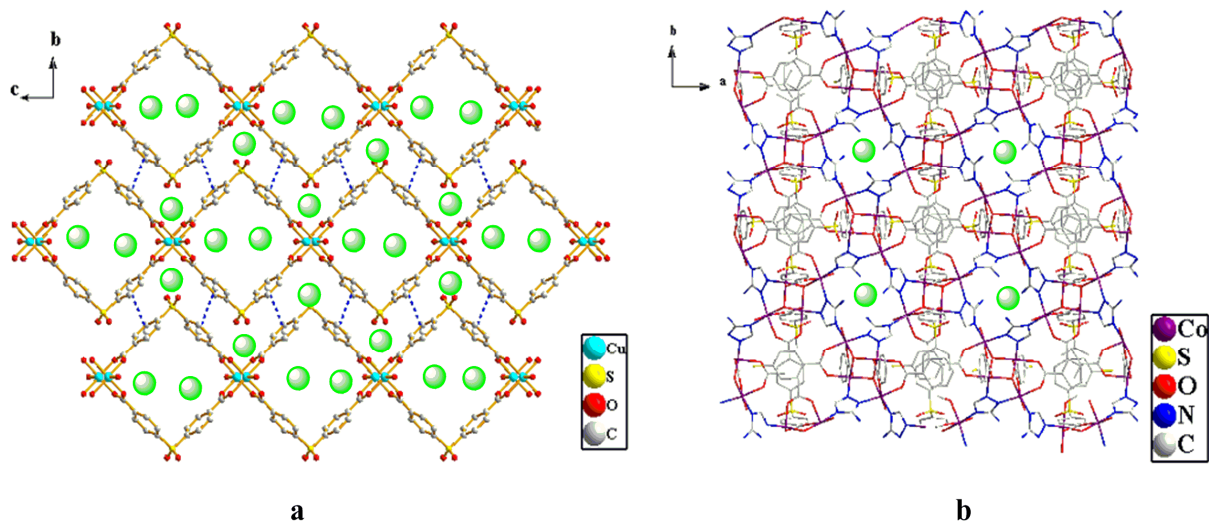


Figure 6. The channels in complexes **5** (a) and **2** (b) are attacked by solvent molecules (the solvent molecules represented as green ball mode).

The same phenomenon had occurred in complexes **5** and **6**. With the introduction of auxiliary ligand Htrz, complex **6** exhibits a 3D “onion” framework and has remarkable chemical resistance to boiling water and organic solvents. Complex **7** was synthesized by the self-assembly of Zn(II) ion, H₂sdba and Hatz. It showed a 3D coordination framework consisting of Zn-triazolate layers and dicarboxylate pillars and indicated a good solvent resistance property. In addition, it was found that **2–4**, **6** and **7** could keep the original shapes for several minutes when the samples were immersed in 0.5 M hydrochloric acid solution or aqueous sodium hydroxide, but **1** and **5** were soluble immediately when the samples were immersed in the acid/base solution.

To confirm whether the crystal structures remained unchanged after treatment, the XRD power patterns for compounds **2** and **7** had been collected on a PANalytical X’prtPro diffractometer using graphite-monochromated Cu K α radiation in the angular range $2\theta = 5-50^\circ$. The powder patterns of compounds **2** and **7** matched with the ones calculated from their single crystal structure data, which indicated that their crystals could retain their crystallinity in boiling water, methanol, ethanol, acetonitrile, and DMF (Figure 7).

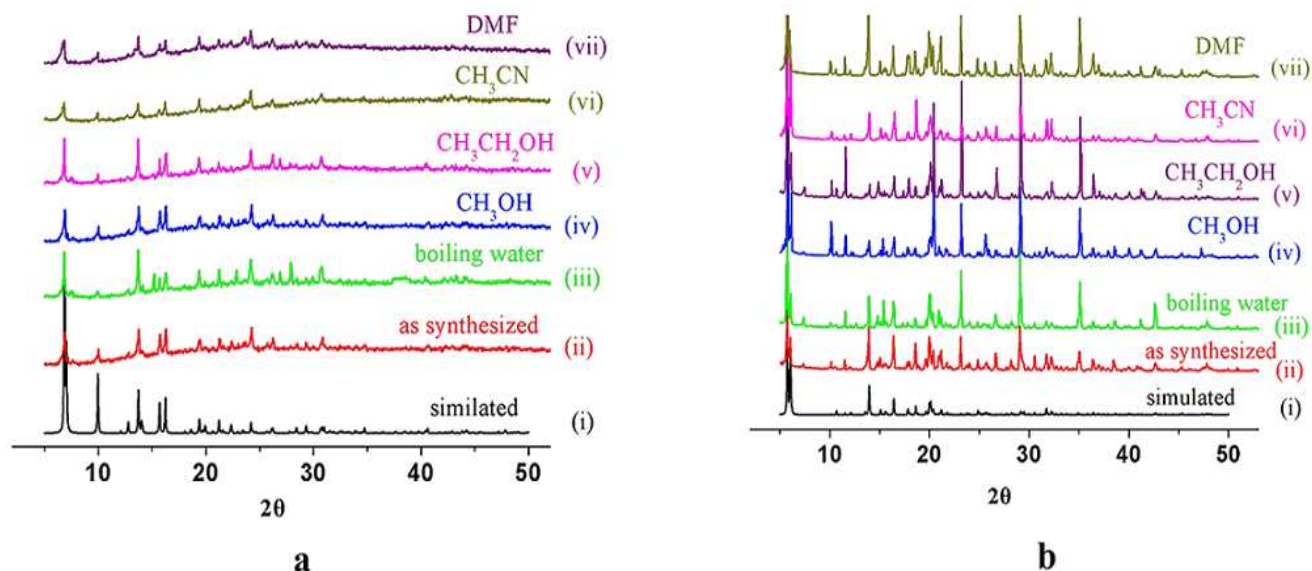


Figure 7. (a) PXRD patterns of **2**: (i) simulated, (ii) as-synthesized, (iii) boiling water, (iv) boiling CH_3OH , (v) boiling $\text{CH}_3\text{CH}_2\text{OH}$, (vi) boiling CH_3CN , (vii) boiling DMF. (b) PXRD patterns of **7**: (i) simulated, (ii) as-synthesized, (iii) boiling water, (iv) boiling CH_3OH , (v) boiling $\text{CH}_3\text{CH}_2\text{OH}$, (vi) boiling CH_3CN , (vii) boiling DMF.

Analyses of the thermal stability. The thermogravimetric analysis (TGA) experiments of **2** and **7** were carried out (Figure S5). The curve of compound **2** shows a weight loss of 6.23% in the 75–320 °C range attributed to the departure of lattice water molecules (calculated 6.59%). After that an additional weight loss of 60.22% up to 533 °C can be attributed to the gradual release of coordinated H_2sdba and Htrz ligands. TG curve of **7** exhibits that it is stable up to 421.3 °C. The thermal stability of **7** is mainly due to the stable 3D coordination framework consisting of Zn-triazolate layers and dicarboxylate pillars. And then, the following weight loss may be attributed to the gradual release of the H_2sdba and Htrz ligands ended at 608 °C with retention of weight of 12.84% (calculated 13.28 %), corresponding to ZnO.

Photoluminescence properties. The fluorescent properties of complexes **2**, **6** and **7**, together with the free H_2sdba ligand, the co-ligands of Htrz and Hatz, were investigated at ambient temperature, as depicted in Figure. S6. The free H_2sdba ligand displays intense emission bands at 329 nm ($\lambda_{\text{ex}} = 277$

nm), which is assigned to the $\pi^* \rightarrow n$ or $\pi^* \rightarrow \pi$ transition.²⁰ As strong electron withdrawing groups, triazole and its derivatives almost have no significant contribution to the fluorescent emission.²¹ Thus, the emission of the coordination polymer is mainly associated with the presence of the H₂sdba ligands.

Complexes **2** and **6** show no detectable fluorescence due to the fact that Co(II)/Cu(II) ion provides an efficient pathway for quenching the fluorescence of the ligand because of the fluorescence quenching nature of paramagnetic Co(II)/Cu(II).²² While complex **7** exhibits an emission maxima at 404 nm ($\lambda_{\text{ex}} = 385$), which is red-shifted 75 nm as compared with the free H₂sdba ligand. Such fluorescence behavior could be due to the metal ion, carboxylate ligand and encapsulated lattice molecule. However, the role of structural complexity and framework robustness can not be ignored. Considering the above factors, it is neither metal-to-ligand charge transfer (MLCT) nor ligand-to-metal charge transfer (LMCT), but it may be assigned to a change in energy levels (HOMO-LUMO) of carboxylate-based ligands. The profile of emission bands suggests the possibility of intraligand ($\pi \rightarrow \pi^*$) transitions.²³

CONCLUSIONS

In summary, we have successfully synthesized and characterized seven new CPs by the self-assembly of H₂sdba, auxiliary ligands (Htrz, Hatz, and Hti), and Co(II), Cu(II), Zn(II) cations under solvothermal conditions. The title complexes display versatile coordination features with 1D, 2D, and 3D frameworks. Therein, with the introduction of rigid organic molecules (Htrz, Hatz, and Hti) as auxiliary ligands, complexes **2-3**, **6** and **7** exhibit interesting 3D frameworks with the first reported topologies **whc1** and **whc2**. The investigation of solvent resistance property had demonstrated that complexes **2-4**, **6** and **7** have more excellent boiling water and organic solvents resistance than that of **1** and **5**. Their excellent solvent resistance property can be ascribed to the rigidity of the linker, dense structure and stable frameworks. In addition, the auxiliary ligands could adopt bridging and bidentate chelating modes to link the center metal ions, decrease the aperture diameters and form hydrogen bond to reduce the

interaction between the solvent and crystal. Herein we have shown a rational approach can be taken toward the construction of CPs with good solvent resistance property and intriguing structural topologies. Actually, there is more work to be done to clarify the intermolecular forces between the solvent and crystal. Further investigations about the solvent resistance property of metal-organic frameworks (MOFs) are currently underway.

Acknowledgment. This work was financially supported by the National Natural Science Foundation (Nos. 21201152 and J1210060).

Supporting Information Available: X-ray crystallographic files in CIF format, selected bond lengths and bond angles, hydrogen bonds of complexes **3**, **4**, and **7**, crystallographic data and structure refinement details for **1–7**. TGA curves for complexes **2** and **7**, the emission spectra of the free ligands and complexes **2**, **6** and **7**.

References

- (1) (a) J. H. Cui, Z. Z. Lu, Y. Z. Li, Z. J. Guo, H. G. Zheng, *CrystEngComm.*, 2012, **14**, 2258. (b) Z. Z. Lu, R. Zhang, Y. Z. Li, Z. J. Guo, H. G. Zheng, *J. Am. Chem. Soc.*, 2011, **133**, 4172. (c) S. S. Chen, M. Chen, S. Takamizawa, P. Wang, C. G. Lv, W. Y. Sun, *Chem. Commun.*, 2011, **47**, 4902. (d) V. A. Russell, C. C. Evans, W. Li, M. D. Ward, *Science.*, 1997, **276**, 575. (e) S. L. James, *Chem. Soc. Rev.*, 2003, **32**, 276. (f) O. R. Evans, W. Lin, *Inorg. Chem.*, 2000, **39**, 2189. (g) B. H. Ye, M. L. Tong, X. M. Chen, *Coord. Chem. Rev.*, 2005, **249**, 545. (h) Z. H. Zhang, C. C. Chen, M. Y. He, Q. Chen, M. Du, *Cryst. Growth Des.*, 2013, **13**, 996. (i) C. Qin, X. L. Wang, E. B. Wang, Z. M. Su, *Inorg. Chem.*, 2008, **47**, 5555.
- (2) (a) A. Czarna, B. Beck, S. Srivastava, G. M. Popowicz, S. Wolf, Y. Huang, M. Bista, T. A. Holak, A. Dömling, *Angew. Chem., Int. Ed.*, 2010, **49**, 5352. (b) K. M. Blake, J. S. Lucas, R. L. LaDuca, *Cryst. Growth Des.*, 2011, **11**, 1287. (c) X. D. Chen, X. H. Zhao, M. Chen, M. Du, *Chem. Eur. J.*, 2009, **15**, 12974. (d) B. S. Zheng, J. F. Bai, J. G. Duan, L. Wojtas, M. J. Zaworotko, *J. Am. Chem. Soc.*,

- 2011, **133**, 748. (e) P. J. Hagrman, D. Hagrman, J. Zubieta, *Angew. Chem., Int. Ed.*, 1999, **38**, 2639. (f) R. Kitaura, K. Fujimoto, S. Noro, M. Kondo, S. Kitagawa, *Angew. Chem., Int. Ed.*, 2002, **41**, 133. (g) Q. Chu, G. X. Liu, Y. Q. Huang, X. F. Wang, W. Y. Sun, *Dalton Trans.*, 2007, 4302.
- (3) (a) P. Horcajada, C. Serre, M. R. Vallet, M. Sebban, F. Taulelle, G. Férey, *Angew. Chem., Int. Ed.*, 2006, **45**, 5974. (b) P. Horcajada, C. Serre, G. Maurin, N. A. Ramsahye, F. Balas, M. Vallet-Regí, M. Sebban, F. Taulelle, G. Férey, *J. Am. Chem. Soc.*, 2008, **130**, 6774. (c) J. S. Hu, L. Qin, M. D. Zhang, X. Q. Yao, Y. Z. Li, Z. J. Guo, H. G. Zheng, *Chem. Commun.*, 2012, **48**, 681. (d) M. P. Suh, H. J. Park, T. K. Prasad, D. W. Lim, *Chem. Rev.*, 2012, **112**, 782. (e) R. Dawson, D. J. Adams, A. I. Cooper, *Chem. Sci.*, 2011, **2**, 1173. (f) T. Wen, D. X. Zhang, J. Zhang, *Inorg. Chem.*, 2013, **52**, 12.
- (4) (a) Z. R. Pan, H. G. Zheng, T. W. Wang, Y. Song, Y. Z. Li, Z. J. Guo, S. R. Batten, *Inorg. Chem.*, 2008, **47**, 9528. (b) X. L. Zheng, Y. Liu, M. Pan, X. Q. Lu, J. Y. Zhang, C. Y. Zhao, Y. X. Tong, C. Y. Su, *Angew. Chem., Int. Ed.*, 2007, **46**, 7399. (c) C. D. Wu, A. G. Hu, L. Zhang, W. B. Lin, *J. Am. Chem. Soc.*, 2005, **127**, 8940. (d) D. S. Li, J. Zhao, Y. P. Wu, B. Liu, L. Bai, K. Zou, M. Du, *Inorg. Chem.*, 2013, **52**, 8091.
- (5) (a) Y. J. Cui, F. F. Yue, G. D. Qian, B. L. Chen, *Chem. Rev.*, 2012, **112**, 1124. (b) L. Brammer, *Chem. Soc. Rev.*, 2004, **33**, 476. (c) M. C. Hong, *Cryst. Growth Des.*, 2007, **7**, 10. (d) S. R. Batten, K. S. Murray, *Coord. Chem. Rev.*, 2003, **246**, 103. (e) S. R. Batten, R. Robson, *Angew. Chem., Int. Ed.*, 1998, **37**, 1460. (f) C. C. Ji, J. Li, Z. J. Guo, Y. Z. Li, H. G. Zheng, *Cryst. Growth Des.*, 2009, **9**, 475. (g) L. Luo, P. Wang, G. C. Xu, Q. Liu, K. Chen, Y. Lu, Y. Zhao, W. Y. Sun, *Cryst. Growth Des.*, 2012, **12**, 2634. (h) Z. Q. Shi, Y. Z. Li, Z. J. Guo, H. G. Zheng, *Cryst. Growth Des.*, 2013, **13**, 3078.
- (6) (a) D. F. Sun, S. Q. Ma, Y. X. Ke, D. J. Collins, H. C. Zhou, *J. Am. Chem. Soc.*, 2006, **128**, 3896. (b) J. A. Zhao, L. W. Mi, J. Y. Hu, H. W. Hou, Y. T. Fan, *J. Am. Chem. Soc.*, 2008, **130**, 15222. (c) J. P. Li, L. K. Li, H. W. Hou, Y. T. Fan, *Cryst. Growth Des.*, 2009, **9**, 4504. (d) Z. Su, M. Chen, T. T. Okamura, M. S. Chen, S. S. Chen, W. Y. Sun, *Inorg. Chem.*, 2011, **50**, 985.
- (7) (a) Z. X. Chen, S. C. Xiang, H. D. Arman, J. U. Mondal, P. Li, D. Y. Zhao, B. L. Chen, *Inorg. Chem.*, 2011, **50**, 3442. (b) L. T. Du, Z. Y. Lu, K. Y. Zheng, J. Y. Wang, X. Zheng, Y. Pan, X. Z. You,

- J. F. Bai, *J. Am. Chem. Soc.*, 2013, **135**, 5622. (c) Y. Huang, T. Liu, J. Lin, J. Lu, Z. Lin, R. Cao, *Inorg. Chem.*, 2011, **50**, 2191.
- (8) (a) C. C. Chen, Z. H. Zhang, Q. Chen, L. Q. Wang, J. Xu, M. Y. He, M. Du, *Chem. Commun.*, 2013, **49**, 1270. (b) D. Farrusseng, S. Aguado, C. Pinel, *Angew. Chem., Int. Ed.*, 2009, **48**, 7502. (c) T. Yang, H. Cui, C. H. Zhang, L. Zhang, C. Y. Su, *Inorg. Chem.*, 2013, **52**, 9053. (d) F. Sun, Z. Yin, Q. Q. Wang, D. Sun, M. H. Zeng, M. Kurmoo, *Angew. Chem., Int. Ed.*, 2013, **52**, 4538.
- (9) (a) J. J. Zhang, L. Wojtas, R. W. Larsen, M. Eddaoudi, M. J. Zaworotko, *J. Am. Chem. Soc.*, 2009, **131**, 17040. (b) A. C. Chamayou, C. Janiak, *Inorg. Chim. Acta.*, 2010, **363**, 2193. (c) Z. Yin, Q. X. Wang, M. H. Zeng, *J. Am. Chem. Soc.*, 2012, **134**, 4857. (d) H. P. Wu, C. Janiak, L. Uehlin, P. Kluefers, P. Mayer, *Chem. Commun.*, 1998, 2637. (e) J. B. Lin, J. P. Zhang, X. M. Chen, *J. Am. Chem. Soc.*, 2010, **132**, 6654. (f) J. F. Eubank, H. Mouttaki, A. J. Cairns, Y. Belmabkhout, L. Wojtas, R. Luebke, M. Alkordi, M. Eddaoudi, *J. Am. Chem. Soc.*, 2011, **133**, 14204. (g) J. H. Luo, H. W. Xu, Y. Liu, Y. S. Zhao, L. L. Daemen, C. Brown, T. V. Timofeeva, S. Q. Ma, H. C. Zhou, *J. Am. Chem. Soc.*, 2008, **130**, 9626. (h) J. L. C. Rowsell, O. M. Yaghi, *J. Am. Chem. Soc.*, 2006, **128**, 1304. (i) S. M. Cohen, *Chem. Rev.*, 2012, **112**, 970.
- (10) (a) T. Li, F. L. Wang, S. T. Wu, X. H. Huang, S. M. Chen, C. C. Huang, *Cryst. Growth Des.*, 2013, **13**, 3271. (b) V. A. Colombo, S. Galli, H. J. Choi, G. D. Han, A. Maspero, G. Palmisano, N. Masciocchi, J. R. Long, *Chem. Sci.*, 2011, **2**, 1311. (c) O. M. Yaghi, O'Keeffe, N. W. M. Ockwig, H. K. Chae, M. Eddaoudi, J. Kim, *Nature.*, 2003, **423**, 705. (d) Y. Han, H. Xu, Y. Y. Liu, H. J. Li, H. W. Hou, Y. T. Fan, S. R. Batten, *Chem. Eur. J.*, 2012, **18**, 13954. (e) Y. Y. Jia, H. J. Li, B. Zhao, Q. Q. Guo, H. W. Hou, Y. T. Fan, *Eur. J. Inorg. Chem.*, 2013, **3**, 438. (f) Y. Y. Jia, H. J. Li, Q. Q. Guo, B. Zhao, Y. Zhao, H. W. Hou, Y. T. Fan, *Eur. J. Inorg. Chem.*, 2012, **18**, 3047. (g) Q. Q. Guo, C. Y. Xu, B. Zhao, Y. Y. Jia, H. W. Hou, Y. T. Fan, *Cryst. Growth Des.*, 2012, **12**, 5439.
- (11) (a) Z. M. Hao, R. Q. Fang, H. S. Wu, X. M. Zhang, *Inorg. Chem.*, 2008, **47**, 8197. (b) C. H. Ke, G. R. Lin, B. C. Kuo, H. M. Lee, *Cryst. Growth Des.*, 2012, **12**, 3758. (c) A. J. Cairns, J. A. Perman, L.

- Wojtas, V. C. Kravtsov, M. H. Alkordi, M. Eddaoudi, M. J. Zaworotko, *J. Am. Chem. Soc.*, 2008, **130**, 1560.
- (12) (a) H. Yuh, H. Satoshi, S. Masayuki, I. Munehiro, F. Tomohiro, K. Susumu, *Inorg. Chem.*, 2013, **52**, 3634. (b) J. D. Lin, X. F. Long, P. Lin, S. W. Du, *Cryst. Growth Des.*, 2010, **10**, 146. (c) C. T. Yeh, W. C. Lin, S. H. Lo, C. C. Kao, C. H. Lin, C. C. Yang, *CrystEngComm.*, 2012, **14**, 1219.
- (13) (a) M. Eddaoudi, D. B. Moler, H. Li, B. Chen, T. M. Reineke, M. O'Keeffe, O. M. Yaghi, *Acc. Chem. Res.*, 2001, **34**, 319. (b) J. R. Li, R. J. Kuppler, H. C. Zhou, *Chem. Soc. Rev.*, 2009, **38**, 1477. (c) D. Sun, S. Ma, Y. Ke, T. M. Petersen, H. C. Zhou, *Chem. Commun.*, (Cambridge, U.K.) 2005, 2663.
- (14) G. M. Sheldrick, *Acta Crystallogr.*, 2008, **A64**, 112.
- (15) Platon Program: A. L. Spek, *Acta Crystallogr., Sect. A* 1990, **46**, 194.
- (16) (a) S. Hayami, K. Murata, D. Urakami, Y. Kojima, M. Akita, K. Inoue, *Chem. Commun.*, 2008, 6510. (b) C. J. Hu, R. M. Chin, T. D. Nguyen, K. T. Nguyen, P. S. Wagenknecht, *Inorg. Chem.*, 2003, **42**, 7602.
- (17) N. Li, L. Chen, F. Y. Lian, F. L. Jiang, M. C. Hong, *Chin. J. Struct. Chem.*, 2009, **28**, 1417.
- (18) (a) T. Loiseau, C. Serre, C. Huguenard, G. Fink, F. Taulelle, M. Henry, T. Bataille, G. Férey, *Chem. Eur. J.*, 2004, **10**, 1373.
- (19) T. Kundu, S. C. Sahoo, R. Banerjee, *Chem. Commun.*, 2012, **48**, 4998.
- (20) (a) S. S. Chen, Y. Zhao, J. Fan, T. Okamura, Z. S. Bai, Z. H. Chen, W. Y. Sun, *CrystEngComm.*, 2012, **14**, 3564. (b) C. Y. Xu, L. K. Li, Y. P. Wang, Q. Q. Guo, X. J. Wang, H. W. Hou, Y. T. Fan, *Cryst. Growth Des.*, 2011, **11**, 4667.
- (21) (a) Y. Bai, G. J. He, Y. G. Zhao, C. Y. Duan, D. B. Dang, Q. J. Meng, *Chem. Commun.*, 2006, 1530. (b) J. P. Zou, Q. Peng, Z. Wen, G. S. Zeng, Q. J. Xing, G. C. Guo, *Cryst. Growth Des.*, 2010, **10**, 2613.
- (22) K. J. Franz, N. Singh, B. Spingler, S. J. Lippard, *Inorg. Chem.*, 2000, **39**, 4081.
- (23) (a) M. Du, X. J. Jiang, X. J. Zhao, *Inorg. Chem.*, 2007, **46**, 3984. (b) M. J. Zaworotko, *Nature.*, 2008, **451**, 410. (c) M. D. Plessis, L. J. Barbour, *Dalton Trans.*, 2012, **41**, 3895.

Table 1. Crystallographic data and structure refinement details for complex **1–7**^{a,b}

| Complex | 1 | 2 | 3 | 4 | 5 | 6 | 7 |
|--|--|--|--|---|---|--|--|
| Formula | C ₅₁ H ₄₉ Co ₃ N ₃ O ₂₃ S ₃ | C ₁₆ H ₁₅ Co ₂ N ₃ O ₉ S | C ₁₆ H ₁₆ Co ₂ N ₄ O ₉ S | C ₂₄ H ₁₉ CoN ₃ O _{8.5} S ₂ | C ₁₄ H ₁₃ CuO ₈ .5S | C ₁₆ H ₁₅ Cu ₂ N ₃ O ₉ S | C ₁₈ H ₁₅ N ₈ O ₆ . ₅ SZn ₂ |
| fw | 1344.93 | 543.23 | 558.25 | 608.48 | 412.85 | 552.46 | 610.24 |
| T/K | 293(2) | 293(2) | 293(2) | 293(2) | 293(2) | 293(2) | 293(2) |
| λ (Mo K), Å | 0.71073 | 0.71073 | 0.71073 | 0.71073 | 0.71073 | 0.71073 | 0.71073 |
| Cryst syst | monoclinic | Tetragonal | Tetragonal | monoclinic | monoclinic | Tetragonal | Orthorhombic |
| Space group | <i>P2(1)/c</i> | <i>I4(1)/a</i> | <i>I4(1)/a</i> | <i>C2/c</i> | <i>C2/m</i> | <i>I4(1)/a</i> | <i>Pbcn</i> |
| <i>a</i> (Å) | 16.654(3) | 25.087(4) | 25.370(10) | 23.564(5) | 12.248(2) | 24.344(3) | 30.671(6) |
| <i>b</i> (Å) | 20.426(4) | 25.087(4) | 25.370(10) | 7.1412(14) | 22.262(5) | 24.344(3) | 16.577(3) |
| <i>c</i> (Å) | 21.802(7) | 15.026(3) | 15.204(3) | 32.254(7) | 7.1435(14) | 15.067(3) | 9.851(2) |
| β (°) | 128.991(18) | 90 | 90 | 105.50(3) | 124.47(3) | 90 | 90 |
| <i>V</i> (Å ³) | 5754(2) | 9457(3) | 9786(6) | 5230.2(18) | 1605.8(6) | 8929(3) | 5008.3(17) |
| <i>Z</i> | 4 | 16 | 16 | 8 | 4 | 16 | 8 |
| <i>D</i> _{calcd.} (g·cm ⁻³) | 1.550 | 1.526 | 1.516 | 1.545 | 1.708 | 1.644 | 1.619 |
| Reflections collected / unique | 10730 / 10730 | 4409 / 4409 | 14539 / 4544 | 4864 / 4864 | 6035 / 1536 | 4390 / 4390 | 4638 / 4638 |
| abs coeff/mm ⁻¹ | 1.038 | 1.533 | 1.485 | 0.864 | 1.521 | 2.043 | 2.048 |
| <i>F</i> (000) | 2596 | 4224 | 4352 | 2368 | 780 | 4288 | 2416 |
| θ (°) | 1.56-25.50 | 1.58-25.50 | 1.56-25.50 | 2.49-25.50 | 1.83-25.49 | 1.67-25.99 | 1.40-25.50 |
| GOF | 1.118 | 1.119 | 1.149 | 1.142 | 1.070 | 1.039 | 1.023 |
| <i>R</i> ₁ (I>2σ(I)) ^a | 0.0939 | 0.0410 | 0.1078 | 0.0623 | 0.0409 | 0.0722 | 0.0505 |
| <i>wR</i> ₂ (I>2σ(I)) ^b | 0.2407 | 0.1055 | 0.2408 | 0.1252 | 0.0950 | 0.1833 | 0.1138 |

$$^a R_1 = \sum ||F_o| - |F_c|| / \sum |F_o|. \quad ^b wR_2 = [\sum w(F_o^2 - F_c^2)^2 / \sum w(F_o^2)^2]^{1/2}.$$

Table 2. Chemical stability of the complexes **1–7** in boiling water, MeOH, EtOH, MeCN, DMF for 48h.

| Solvent Complex | Boiling water | MeOH | EtOH | MeCN | DMF |
|--------------------|------------------|-----------|-----------|-----------|-----------|
| 1 | -- | stability | stability | stability | stability |
| 2 | stability | stability | stability | stability | stability |
| 3 | stability | stability | stability | stability | stability |
| 4 | stability | stability | stability | stability | stability |
| 5 | stability | -- | -- | stability | -- |
| 6 | stability | stability | stability | stability | stability |
| 7 | stability | stability | stability | stability | stability |

Captions for Figures

Scheme 1. Schematic molecular structure of H₂sdba and bix ligands.

Figure 1. (a) Coordination environments of the Co(II) ions in **1**. Hydrogen atoms are omitted for clarity. (b) The coordination mode of sdba²⁻ and secondary building unit (SBU). (c) The 2D sheet are connected by Co1 (pink) to form a 3D framework. (d) Topological structure of the 3D framework.

Figure 2. (a) Coordination environments of the Co(II) ions in **2**. Hydrogen atoms are omitted for clarity. (b) The tetranuclear cobalt (II) cluster. (c) Connectivity between two sheets through trz⁻ unit to form the 3D framework along the *c* axis. (d) Schematic view of the {3⁶.4¹⁰.5⁶.6⁶} topology (the tetranuclear cobalt cluster represented as rose red ball mode).

Figure 3. (a) Coordination environments of the Co(II) ions in **4**. Hydrogen atoms are omitted for clarity. (b) View of 1D helical chain along *a* axis. (c) View of the 2D network of compound **4** along *b* axis. The inter-chain strong hydrogen bonds are represented by dashed lines.

Figure 4. (a) An infinite 1D ∞-like chains formed by Cu(II) cation centers and sdba²⁻ ligands. Hydrogen atoms are omitted for clarity. (b) View of the 2D network of compound **5** down *a* axis. The weak π⋯π stacking interactions are represented by dashed lines.

Figure 5. (a) Coordination environments of the Zn(II) ions in **7**. Hydrogen atoms are omitted for clarity. (b) View of the 2D network formed by atz⁻ ligands and Zn(II) cations in **7**. (c) Connectivity between two networks through sdba²⁻ unit to form the 3D framework along the *c* axis. (d) Schematic representation of 4-connected topology of **7** (purple nodes: Zn; yellow nodes: Hatz ligands).

Figure 6. The channels in complexes **5** (a) and **2** (b) are attacked by solvent molecules (the solvent molecules represented as green ball mode).

Figure 7. (a) PXRD patterns of **2**: (i) simulated, (ii) as-synthesized, (iii) boiling water, (iv) boiling CH₃OH, (v) boiling CH₃CH₂OH, (vi) boiling CH₃CN, (vii) boiling DMF. (b) PXRD patterns of **7**: (i) simulated, (ii) as-synthesized, (iii) boiling water, (iv) boiling CH₃OH, (v) boiling CH₃CH₂OH, (vi) boiling CH₃CN, (vii) boiling DMF.

Seven Dicarboxylate-Based Coordination Polymers with Structural Varieties and Solvent Resistance Property Changing Derived from the Introduction of Small Organic Linkers

Chao Huang, Feixiang Ji, Lu Liu, Na Li, Haofei Li, Jie Wu*, Hongwei Hou*, Yaoting Fan

Introducing organic molecules as coligands, several coordination polymers with new topologies and remarkable solvents resistance property have been obtained.

